$$\frac{Ng^2\mu_\beta^2}{2kT} = \frac{60 + 28\exp(-4x) + 10\exp(-7x) + 2\exp(-9x)}{9 + 7\exp(-4x) + 5\exp(-7x) + 3\exp(-9x) + \exp(-10x)} \quad (9)$$

best fit parameters are $J = -3.55$ cm^{-1} and $g = 1.95$ with an R value of 0.8%. The deviation of the fit at low temperature (<10 K) is a result of the asymmetry of the dimer. The relatively low g value is a good indication of this structural asymmetry and large zero-field splitting.

Conclusion

Manganese(III) Schiff base complexes provide a rich series of structural types that can be used as models for the magnetic and structural properties of manganoenzymes. The propensity of manganese to form carboxylate-bridged clusters suggests that amino acids such as aspartate and glutamate may provide structural integrity to biological manganese clusters. The $Mn^{III}_2Mn^{II}(SALADHP)_2(OAc)_4(CH_3OH)_2$ complexes in both linear[28] and bent[29] geometries clearly document this tendency. The isolation of **5** extends the range of structures in this family to mixed manganese–alkali-metal cation complexes. Alkaline-earth ions also promote the formation of loosely associated clusters.[44] This observation, taken together with biophysical studies of higher plant photosynthesis, may provide insight toward the structure of the manganese cluster(s) involved in biological water oxidation. A strict calcium requirement is observed for both oxygen-evolving activity and production of the S_2 state multiline signal of the thylakoid membrane associated oxygen-evolving complex (OEC) of photosystem II.[45,46] It is also known that sodium competes for at the least one of the calcium binding sites in the OEC.[47] The D1 and D2 peptides, which most likely contain the manganese ions, are rich in carboxylate residues.[48] Thus, it is quite possible that the calcium functions to provide stability to the manganese cluster in higher oxidation states.[46] This stability may be imparted through stabilization of the protein structure by a direct association with the cluster via carboxylate bridges as observed for concanavalin A.[49] Complex **5** provides an example of how such a redox-inactive metal could promote manganese cluster formation.

Acknowledgment. V.L.P. thanks the Chicago Community Trust/G.D. Searle Scholars Program for a Biomedical Research Scholarship. J.A.B. acknowledges a postdoctoral research fellowship from the Program for Protein Structure and Design (University of Michigan). M.L.K. and W.E.H. wish to acknowledge support by the National Science Foundation (Grant No. CHE-8807498). The technical assistance of Erlund Larson was greatly appreciated.

Registry No. **1**, 120205-66-5; **2**, 120204-38-8; **3**, 120204-54-8; **4**, 120294-48-6; **5**, 120229-27-8; salicylaldehyde, 90-02-8; 1,3-diamino-2-hydroxypropane, 616-29-5; 5-chlorosalicylaldehyde, 635-93-8.

Supplementary Material Available: Tables IX, XIV, and XIX (anisotropic thermal parameters for all non-hydrogen atoms), Tables X, XV, and XX (complete list of bond lengths), Tables XI, XVI, and XXI (complete list of bond angles), and Tables XII, XVII, and XXII (fractional coordinates for hydrogen atoms) for complexes **1**, **4**, and **5**, respectively, and Table XXIV (X-ray powder d spacings in Å) for complexes **1** and **4** (12 pages); Tables XIII, XVIII, and XXIII (F_o vs F_c) for complexes **1**, **4**, and **5**, respectively (30 pages). Ordering information is given on any current masthead page.

(44) Fenton, D. E.; Bresciani-Pahor, N.; Calligaris, M.; Nardin, G.; Randaccio, L. *J. Chem. Soc., Dalton Trans.* **1979**, 39.
(45) Carumarata, K.; Cheniae, G. M. *Plant Physiol.* **1987**, *84*, 587.
(46) Ghanotakis, D. F.; Topper, J. N.; Babcock, G. T.; Yocum, C. F. *FEBS Lett.* **1984**, *170*, 169.
(47) Waggoner, C.; Pecoraro, V. L.; Yocum, C. F. *FEBS Lett.* **1989**, *244*, 237.
(48) Trebst, Z. *Z. Naturforsch.* **1986**, *41C*, 240.
(49) Hardman, K. D.; Ainsworth, C. F. *Biochemistry* **1972**, *11*, 4910.

Contribution from the Departments of Chemistry, The University of Michigan, Ann Arbor, Michigan 48109, and University of Massachusetts, Amherst, Massachusetts 01003

Structurally Diverse Manganese(III) Schiff Base Complexes: Solution Speciation via Paramagnetic ^{1}H NMR Spectroscopy and Electrochemistry

Joseph A. Bonadies,[1] Michael J. Maroney,*[,2] and Vincent L. Pecoraro*[,1,3]

Received September 2, 1988

The mononuclear cation $Mn(2\text{-OH-SALPN})^+$ (2-OH-SALPN = dianion of *N,N'*-disalicylidene-2-hydroxypropanediamine) converts cleanly to a novel monoalkoxy-bridged dimer, $Mn^{III}_2(2\text{-OH-SALPN})_2$(solvent), by the stoichiometric addition of sodium methoxide or tetrabutylammonium hydroxide in methanol, DMF, or acetonitrile. This conversion, which involves deprotonation of the ligand alcohol group, can be followed by using cyclic voltammetry and ^{1}H NMR spectroscopy. The monomer undergoes reduction [Mn(III/II)] at −182 mV vs SCE in methanol. The Mn(III) dimer has metal-based oxidations at +230 and +1600 mV. Comparison of these redox processes with those of the structurally related mononuclear Mn(IV) complex $Mn(SALADHP)_2$ [SALADHP = dianion of 2-methyl-2-(salicylideneamino)-1,3-dihydroxypropane] indicates that the Mn(IV) oxidation state has been destabilized by nearly 700 mV in the dimer by the presence of a bridging alkoxide ligand. Both the monomer and dimer give rise to isotropically shifted ligand proton NMR resonances due to the presence of paramagnetic high-spin Mn(III) centers. With use of ring-substituted derivatives, the hyperfine shifted resonances have been assigned to specific ligand protons. The ^{1}H NMR spectrum obtained for the monomer consists of relatively sharp peaks assigned to phenolate protons at −21.9 (5′-H) and −23.8 (4′-H) ppm and a broad resonance at +28.1 ppm that is assigned to the proton on the 2-carbon atom of the propane backbone. The resonance due to this last proton is absent from the spectrum of the dimer, which exhibits phenolate proton resonances at −3.4 (6′-H), −5.3 (4′-H), and −13.7 (5′-H) ppm. This information has allowed characterization of species in solution, including a trinuclear complex, $[NaMn^{III}_2(2\text{-OH-SALPN})_2(OAc)_4]^-$, which forms both the monomeric cation and dimer in solution.

Introduction

It is now recognized that manganese plays an important role in numerous redox processes associated with the metabolism of dioxygen. This has prompted recent attempts to understand the coordination chemistry of Mn(III) ions, which are now believed to play a role in at least three enzymes: manganese superoxide dismutase (MnSOD),[4] manganese catalase,[5] and the photosyn-

(1) The University of Michigan.
(2) The University of Massachusetts.
(3) G. D. Searle Biomedical Research Scholar (1986–1989), Alfred P. Sloan Fellow (1989–1991).
(4) Recent reviews that discuss these points are: Pecoraro, V. L. *Photochem. Photobiol.* **1988**, *48*, 249. Babcock, G. T. Photochemistry. In *New Comprehensive Biochemistry*; Amesz, J., Ed.; Elsevier: Amsterdam, 1987; Vol. 15, p 125.

0020-1669/89/1328-2044$01.50/0

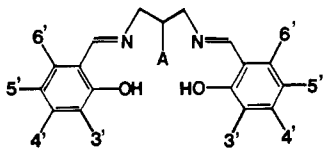

Figure 1. Ligands used in this study:

Ligand	in complex	2	3'	4'	5'	6
SALPN	4	H	H	H	H	H
2-OH-SALPN	1, 2, 3	OH	H	H	H	H
2-OH-(3,5-Cl-SAL)PN	7, 8	OH	Cl	H	Cl	H
2-OH-(4-OMe-SAL)PN	11, 12	OH	H	OMe	H	H
2-OH-(5-Cl-SAL)PN	5, 6	OH	H	H	Cl	H
2-OH-(5-Br-SAL)PN	9, 10	OH	H	H	Br	H
2-OH-(5-OMe-SAL)PN	13, 14	OH	H	H	OMe	H
2-OH-(6-OMe-SAL)PN	15, 16	OH	H	H	H	OMe

thetic oxygen-evolving complex (OEC).[6-8] In the last case, considerable controversy surrounds the oxidation states and nuclearity of the active-site manganese ions, with mono-, di-, tri-, and tetrameric formulations having been advanced.[6]

Manganese(III) imino phenolates have modeled some of the chemistry of these biological sites. Complexes that catalytically oxidize water to dioxygen when exposed to intense visible light have been reported.[9] The acidification of bis(μ-oxo) Mn(IV) imino phenolates leads to the quantitative production of hydrogen peroxide.[10] Dimers have been implicated in these model systems; however, proof of structure of reactive species has been inconclusive due to difficulties associated with spectroscopic studies of Mn(III). These difficulties include the lack of an EPR signal at X-band frequencies and weak d–d transitions ($\epsilon < 500$ M^{-1} cm^{-1}) in the electronic absorption spectra.

High-spin Mn(III), in an octahedral field, has a ^5E electronic ground state and is expected to show well-resolved, isotropically shifted ^1H NMR spectra arising from ligand protons.[11] In fact, spectra have been obtained for Mn(III) porphyrins[12] and for dinuclear Mn^{III}_2 complexes, $[Mn(HB(pz)_3)]_2O(O_2CR)_2$ [$HB(pz)_3$ = tripyrazolylhydroborate].[13] In this contribution we apply ^1H NMR spectroscopy of isotropically shifted phenolate proton resonances, electrochemical techniques, and magnetic susceptibility and conductivity measurements to examine the solution speciation of Mn(III) complexes of the dianion of the Schiff base ligand *N,N'*-disalicylidene-2-hydroxypropanediamine (2-OH-SALPN) (Figure 1), which is shown to dimerize under basic conditions to give a crystallographically characterized,[14] neutral, alkoxy-bridged dimer. As a result of these studies, we provide the first example of the use of high-spin Mn(III) ions to perturb the proton resonances of phenolate ligands. This information suggests the possible application of ^1H NMR to examine the active-site structure of manganoenzymes.

Experimental Section

Materials. Salicylaldehyde (SAL), 5-bromosalicylaldehyde (5-Br-SAL), and 1,3-diamino-2-hydroxypropane were obtained from Aldrich Chemical Co. 3,5-Dichlorosalicylaldehyde (3,5-Cl_2-SAL) and 5-chlorosalicylaldehyde (5-Cl-SAL) were obtained from Pfaltz and Bauer. 2-Amino-2-methyl-1,3-propanediol, $Mn(CH_3COO)_3\cdot 2H_2O$, and $Mn(CH_3COO)_2\cdot 2H_2O$ were obtained from Fluka Co. Tetra-*n*-butylammonium hexafluorophosphate [(TBA)PF_6] was synthesized by the metathesis of (TBA)Br and NH_4PF_6 in water followed by three recrystallizations from absolute ethanol. For the electrochemical studies, high-purity solvents [methylene chloride, dimethylformamide (DMF), and methanol] were used as received from American Burdick and Jackson Co. High-purity argon gas was used to deoxygenate solutions. All other chemicals and solvents were reagent grade.

Ligands and Complexes. $[Mn(2\text{-}OH\text{-}SALPN)(OAc)]_n$ (**1**), $Mn_2(2\text{-}OH\text{-}SALPN)_2(CH_3OH)\cdot CH_3OH$ (**2**), Mn(2-OH-SALPN)(NCS) (**3**), $Mn_2[2\text{-}OH(5\text{-}Cl\text{-}SAL)PN]_2(CH_3OH)\cdot CH_3OH$ (**6**), and $[C_2H_9O_2][NaMn_2(2\text{-}OH\text{-}SALPN)_2(OAc)_4]\cdot 2H_2O$ (**17**) were synthesized as described in the preceding paper (numbered **1**, **3**, **2**, **4**, and **5**, respectively).[14] Substituted analogues Mn[2-OH(5-Cl-SAL)PN](NCS) (**5**), Mn[2-OH-(3,5-Cl_2-SAL)PN](NCS) (**7**), $Mn_2[2\text{-}OH(3,5\text{-}Cl_2\text{-}SAL)PN]_2(CH_3OH)\cdot CH_3OH$ (**8**), Mn[2-OH(5-Br-SAL)PN](NCS) (**9**), and $Mn_2[2\text{-}OH(5\text{-}Br\text{-}SAL)PN]_2(CH_3OH)\cdot CH_3OH$ (**10**) were all synthesized by the same routes that produced **2** and **3** for mono- and binuclear complexes, respectively, with use of the appropriately substituted aldehyde. The mononuclear cations and binuclear complexes of the 4-, 5-, and 6-methoxy-substituted analogues of 2-OH-SALPN were all generated as dimers. All studies on the mononuclear complexes involved in situ generation by stoichiometric addition of perchloric acid. The mononuclear and binuclear complexes for these ligands are numbered as 4-OMe (**11** and **12**), 5-OMe (**13** and **14**), and 6-OMe (**15** and **16**), respectively. Each substituted complex was identified by its IR and electrochemical behavior. $[Mn(SALPN)H_2O]ClO_4$ (**4**) was synthesized by literature methods.[9]

Methods. ^1H NMR spectra of the model complexes were obtained on a Bruker 360-MHz FT-NMR spectrometer operating in the quadrature detection mode (^1H frequency 360.1 MHz). Spectra were collected by using a one-pulse sequence with a 90° pulse of 9.9 μs. Between 3000 and 10000 transients were accumulated over a 50-kHz bandwidth for each sample. The spectra contained 8K data points, and the signal to noise ratio was improved by apodization of the free induction decay, which introduced a negligible 10–20-Hz line broadening. Chemical shifts were referenced to TMS or resonances due to residual protons present in the deuterated solvents.

UV–visible spectra were recorded on a Perkin-Elmer Lambda 9 UV/vis/near-IR spectrophotometer equipped with a Perkin-Elmer 3600 data station. Infrared spectra were obtained on a Nicolet 60-SX FT-IR instrument as KBr pellets. Solid-state magnetic susceptibilities were determined by using a Johnson-Matthey magnetic susceptibility balance (MSB-1), using $Hg[Co(SCN)_4]$ as a calibration standard. Solution magnetic susceptibilities were determined by using the Evans method[15,16] and a 360-MHz Bruker FT-NMR spectrometer. Magnetic moments from both methods are reported on a per manganese basis unless otherwise specified. Conductivity measurements were performed on a Beckman Model RC-16C conductivity bridge utilizing a dip cell. Chemical analyses were performed by either Galbraith Laboratories, Inc., Knoxville, TN, or Oneida Research Services, Inc., of White Plains, NY.

Cyclic voltammetry and bulk electrolysis studies were completed on a Bioanalytical Systems BAS-100 electrochemical analyzer. Cyclic voltammograms were generated by using platinum-bead, platinum-wire, and saturated calomel (SCE, within a Luggin probe) electrodes as the working, auxiliary, and reference electrodes, respectively, in a three-electrode configuration. Bulk electrolyses utilized either a platinum basket or platinum screen for working and auxiliary electrodes, each being separated by a fine frit. Tetrabutylammonium hexafluorophosphate [(TBA)PF_6] was used as the supporting electrolyte at 0.1 M concentration. All potentials are reported vs the ferrocene/ferrocenium couple empoyed as an external reference.

Results and Discussion

Manganese complexes of 2-OH-SALPN have been synthesized as monomeric, dimeric, polymeric, and cage complexes. The structures and magnetic properties of these compounds in the solid state were described in the previous paper in this journal.[14] The spectroscopic properties of Mn complexes, as well as those of biological Mn complexes, are often measured in solution. Thus, it becomes imperative that the solution behavior of the compounds

(5) Ludwig, M. L.; Pattridge, K. A.; Stallings, W. C. *Manganese in Metabolism and Enzyme Function*; Academic Press: New York, 1986; p 405.
(6) Beyer, W. F., Jr.; Frodovich, I. *Manganese in Metabolism and Enzyme Function*; 1986 Academic Press: New York, 1986; p 193.
(7) Asmez, J. *Biochem. Biophys. Acta* **1983**, *726*, 1.
(8) Dismukes, G. C. *Photochem. Photobiol.* **1986**, *43*, 99.
(9) Ashmawy, F. W.; McAuliffe, C. A.; Parish, R. V.; Tames, J. *J. Chem. Soc., Dalton Trans.* **1985**, 1391.
(10) Boucher, L. J.; Coe, C. G. *Inorg. Chem.* **1975**, *14*, 1289.
(11) Swift, T. J. In *NMR of Paramagnetic Molecules*; Lamar, G. N., Horrocks, W. D., Jr., Holm, R. H., Eds.; Academic Press: New York, 1973; p 53.
(12) Goff, H. M.; Hansen, A. P. *Inorg. Chem.* **1984**, *23*, 321.
(13) Sheats, J. E.; Czernuszewicz, R. S.; Dismukes, G. C.; Rheingold, A. L.; Petrouleas, V.; Stubbe, I.; Armstrong, W. M.; Lippard, S. J. *J. Am. Chem. Soc.* **1987**, *109*, 1435.
(14) Bonadies, J. A.; Kirk, M. L.; Lah, M. S.; Kessissoglou, D. P.; Hatfield, W. E.; Pecoraro, V. L. *Inorg. Chem.*, preceding paper in this issue.
(15) Evans. D. F. *J. Chem. Soc.* **1959**, 2003.
(16) Bartle, K. D.; Dale, B. J.; Jones, D. W.; Maricic, J. *J. Magn. Reson.* **1973**, *12*, 286.

Table I. Paramagnetic NMR Shifts

complex no. and conditions	shifts (vs 0 ppm)					
			Methanol-d_4			
1	+28.6 (b)[b]	[−3.5][a]	[−5.8]	[−14.2]	−21.7	−23.8
2		−3.4	−5.3	−13.7		
2 + $^1/_2$ equiv of acid	+28.3 (b)	−3.5	−5.3	−13.7	−21.7	−23.7
3	+28.1 (b)				−21.9	−23.8
3 + $^1/_2$ equiv of base	+28.4 (b)	−3.4	−5.3	−13.8	−21.9	−23.8
3 + 1 equiv of base		−3.4	−5.3	−13.7		
3 + 1 equiv of acid[c]	+28.4 (b)				−21.7	−23.7
4	+19.0 (b)				−22.6	−25.0
5	+26.9 (b)				−20.0	
6		−4.5				
7	+29.3 (b)				−16.9	
8		−2.1				
9	+28.9 (b)				−19.9	
10		−4.6				
11 (in situ)	+30.3 (b)				−21.7	
12		−2.0		−14.7		
13 (in situ)	+25.9 (b)				−22.7	
14		−5.8 (b)	−7.0			
15 (in situ)	+28.3 (b)				−21.7	−26.7
16		−4.0	−17.0			
17	+28.6 (b)	−3.5	−5.8	−14.0	−21.6	−23.5
Mn(SALEN)X		−4.2 (b)			−23.2	−29.0
			DMF-d_7			
1		−4.6	−5.9	−16.6	−18.3	
1 + MeOH		−5.9		−16.2	−21.3	−22.9
1 + acid (HOAc)					−21.9	
2		−4.3	−5.6	−16.3		
2 + $HClO_4$	+25.4 (b)				−20.5	−22.3
3	+23.9 (b)				−21.6	
3 + NaOAc	+24.7 (b)	−4.4	−5.6	−16.2	−19.4	
4	+18.2 (b)				−20.8	−22.4
5	+25.6 (b)				−18.1	
6		−3.5	−5.9			
7	+26.8 (b)			−14.3		
8		−1.9 (b)				
9	+25.6 (b)				−18.5	
10		−2.1 (b)				
11	+26.2 (b)				−20.6	
12		−4.8			−17.4	
13	+25.0 (b)				−19.2	
14		−4.5				
15					−17.1	−22.3
16		−1.8		−16.9		
17	+24.9 (b)	−3.8	−5.1	−15.7	−17.1	
Mn(SALEN)X	+30.4 (b)				−22.9	−24.1
			CD_3CN			
2		−3.3	−7.1	−17.7		
6		−2.5	−7.4			
10		−3.8	−8.7			

[a] Brackets indicate very small peaks. [b] b indicates a broad peak. [c] Acid added subsequent to the above base. In situ spectra were generated by acid addition to the corresponding dimers.

be understood. A perpetual concern of synthetic chemists is the assignment of solution structure based on X-ray crystallographic studies of the solid state. Extrapolation to the solution structure is particularly risky in clusters that are formed through the loose association of ions. Toward this end, we examined the magnetic, conductivity, electrochemical, and ^1H NMR and electronic absorption spectroscopic properties of solutions of this family of compounds. The observation of a number of isotropically shifted ligand proton resonances in the ^1H NMR spectra of these materials has proven to be particularly valuable in the characterization of solution speciation. The results of these studies are reported in Tables I–IV.

NMR Studies. The ^1H NMR spectra obtained for the unsubstituted monomer Mn(2-OH-SALPN)(NCS) (**3**), which forms the monomeric cation Mn(2-OH-SALPN)$^+$ in solution (vide infra), and various ring-substituted derivatives in CD_3OD are shown in Figure 2. The corresponding numerical data are contained in Table I. The spectrum obtained for the unsubstituted monomer contains three proton resonances that lie outside the diamagnetic region (ca. 0–10 ppm). Two relatively sharp peaks are observed upfield (−21.9 and −23.8 ppm), and one broad peak is observed downfield (+28.1 ppm). It is possible to assign the upfield proton resonances to the 4′- and 5′-protons of the ring using ring-substituted derivatives. Substitution of chlorine in the 5-position of the phenolate rings results in a spectrum with features at +26.9 and −20.0 ppm. Clearly one of the upfield peaks arises from the 5′-H atom. Two features are again present when the spectrum of the 3,5-dichloro analogue is examined. The downfield resonance is still observed, as is a peak at −16.9 ppm. Substitution of the 4′-, 5′-, and 6′-positions of the ring with −OMe provides a clear indication of the appropriate assignments. Substitution at the 4′- and 5′-positions yield spectra containing a single upfield resonance, while substitution in the 6′-position gives rise to the observation of two upfield resonances. In all cases, a resonance is observed at 28 ± 2 ppm; thus, the downfield resonance cannot arise from a phenolate proton. The upfield peaks in the spectrum of the unsubstituted complex must arise from the 4′- and 5′-protons of the ring (−23.8 and −21.9 ppm, respectively), and the protons

Table II. Magnetic Moments of Manganese Complexes

compd no.	solid state μ_{eff}, μ_B	solution solvent and solutes	solution μ_{eff},[a] μ_B	conductivity
1	4.85	DMF	4.63	0
		+ acid	5.05	
		+ base	4.63	
		MeOH	5.01	1:1
		+ NaOAc	4.50	
		+ base	4.46	
2	4.76 [6.73]	DMF	4.82 [6.81]	0
		+ acid	5.09	
		+ base	4.67 [6.61]	
		MeOH	4.92 [6.96]	≪1:1
		+ acid	5.16	
		+ base	4.89 [6.92]	
3	5.02	DMF	4.94	1:1
		+ base	4.71	
		MeOH	4.94	1:1
		+ NaOAc	4.68	
		+ base	4.55	
8	4.85 [6.86]	DMF	4.86 [6.87]	0[b]
		+ acid	5.37	
17	5.01 [7.08]	DMF	4.85 [6.83]	1:1
		+ acid	5.16	
		MeOH	5.35 [7.54]	>1:1
		+ acid	5.39	

[a] Per manganese ion. Numbers in brackets are per complex. [b] Also a nonelectrolyte in methanol; not sufficiently soluble in methanol for solution magnetic determination.

Table III. Electrochemical Properties[a]

compd no.	ox/red[b]	E_{pa}	E_{pc}	I_{pa}	I_{pc}
		Methanol			
1	R	−0.088	−0.178	2.88	1.92
	O	+0.307	+0.213	0.13	0.04
2	O	+0.314	+0.236	1.15	0.98[b]
3	R	−0.085	−0.182	1.96	2.40
17	R	−0.086	−0.176	2.52	1.83
	O	+0.310	+0.233	0.21	0.09
		DMF			
1	O	+0.293	+0.199	0.63	0.62
2	O	+0.268	+0.169	1.19	1.13[b]
3	R	−0.104	−0.217	1.22	1.98
17	O	+0.282	+0.147	0.71	0.48
	O′	+0.517	+0.409	0.79	0.59

[a] Data was obtained on ~1 mM samples, at a scan rate of 100 mV/s. All E values are in V and I values in mA. [b] Oxidative and reductive processes confirmed by rotating platinum electrode voltammetry.

Table IV. UV-Visible Spectroscopic Properties[a]

complex no.	MeOH	DMF
1	375 (9640), 277 (25 960), 233 (43 020)	386 (9520), 265 (35 220)
2	383 (14 100), 268 (53 000), 234 (73 900)	388 (17 820), 266 (67 900)
3	375 (7700), 279 (20 640), 232 (35 000)	376 (81 320), 274 (21 940)
17	375 (18 660), 277 (51 780), 234 (85 690)	383 (16 970), 264 (61 350)

[a] Data are presented as wavelength in nm (ϵ in M^{-1} cm^{-1}). Extinction coefficient data are calculated on a per complex basis.

"ortho" to a ring position occupied by a Mn-donor atom are not observed. The assignment of the 4′- and 5′-protons of the ring is based on the stepwise chemical shift charge of the −23.8 ppm peak in the 5-chloro and 3,5-dichloro analogues (**5** and **8**) and the same chemical shift for the −21.9 ppm peak in the 4-OMe-substituted analogue **11**.

The downfield resonance is assigned to the proton on the 2-C atom of the propane backbone on the basis of the examination of the ^1H NMR spectra of structurally related complexes. The

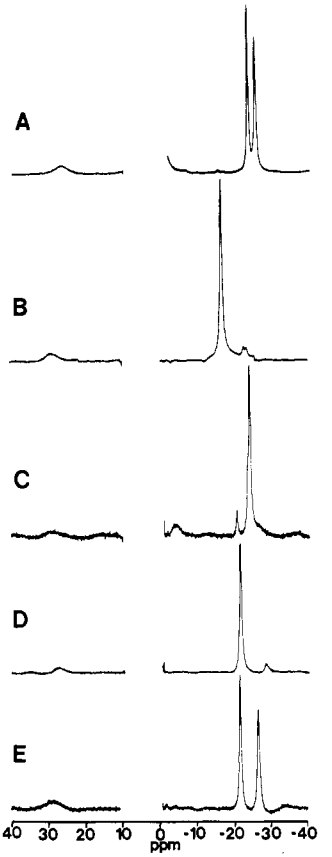

Figure 2. Paramagnetic NMR spectra of the mononuclear complexes of this study in CD_3OD. Spectra A–E represent complexes **3**, **7**, **13**, **11**, and **15**, respectively.

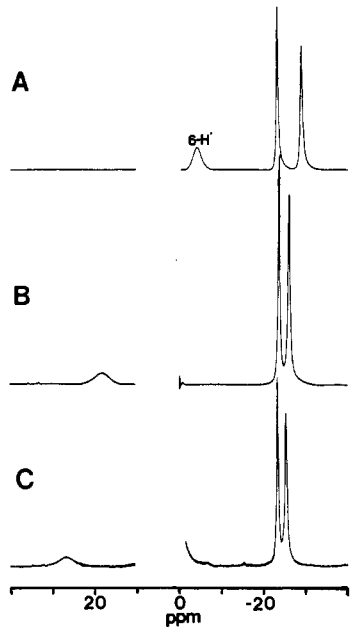

Figure 3. Paramagnetic NMR spectra of mononuclear manganese complexes containing different backbones. Spectra A–C represent complexes $Mn(SALEN)^+$, **4**, and **2**, respectively. CD_3OD is the solvent in each case.

spectrum obtained for Mn(SALEN)X [SALEN = *N*,*N*′-ethylenebis(salicylideneamine)], which features an ethane backbone, does not show a peak shifted downfield (Figure 3A, Table III). However, the spectrum of $[Mn(SALPN)H_2O]ClO_4$ [**4**; SALPN = *N*,*N*′-propylenebis(salicylideneamine); Figure 3B, Table III], with an unsubstituted propane backbone, does display a low-field resonance. The assignment of the downfield resonance to the 2-C proton is also consistent with the absence of this peak

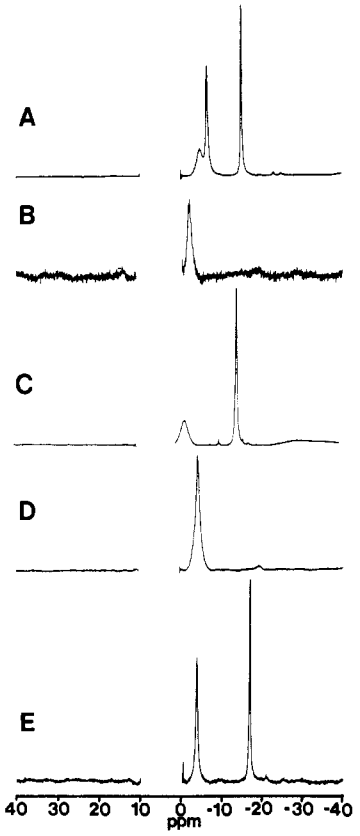

Figure 4. Paramagnetic NMR spectra of the dinuclear complexes of this study in CD_3OD. Spectra A–E represent complexes **2**, **6**, **12**, **8**, and **16**, respectively.

in the spectra obtained for the alkoxy-bridged dimeric complexes (vide infra).

The isotropic shifts of the Fe(SALEN)X family of complexes[17] are very sensitive to the axial ligand X. In contrast, identical ^1H NMR spectra of Mn(SALEN)X are obtained when X = NCS^-, Cl^-, or substituted phenolates. This suggests that in solution the axial ligand dissociates to form $Mn(SALEN)^+$. This is confirmed by the solution conductivity, which shows Mn(SALEN)X to be a 1:1 electrolyte. In addition, the UV–visible spectra and cyclic voltammograms are also invariant with X group. Identical chemistry has been observed for the Mn(2-OH-SALPN)X complexes reported herein.

The data obtained for the analogous dimeric complexes are summarized in Table I and illustrated as Figure 4. The unsubstituted dimer **2** [Mn_2(2-OH-SALPN)$_2$(CH_3OH)] may be synthesized by analogy with 5-chloro-substituted analogue **6**, whose structure was reported in the previous paper.[14] The spectrum of the unsubstituted dimer in CD_3OD displays only upfield resonances (−3.5, −5.3, and −13.7 ppm). These resonances are in the range previously seen for other manganese(III) dimers[13] (+67 > δ > −56 ppm). Ring substitution at the 6′-position removes the broader resonance at −3.5 ppm without greatly perturbing the remaining two sharper resonances. The peak at −5.3 ppm is lost upon substitution at the 4′-position, and the resonance at −13.7 ppm is absent from the spectra of the derivatives substituted at the 5′-position. Thus, the three peaks observed in the spectrum of the parent complex may be assigned to the phenolate ring protons in the 6′-, 4′-, and 5′-positions, with respect to increasing upfield shift. The 3′-H is not observed, nor are the spectra greatly perturbed by substitutions at the 3′-position. The fact that the observed isotropic shifts for the 4′- and 5′-H resonances are less than in the monomers is consistent with a small degree of antiferromagnetic coupling between the Mn centers in the dimers (Table II). The two resonances arising from the 6′- and 4′-H atoms are seen to coalesce in the 5′-substituted complexes in CD_3OD but are resolved in CD_3CN. The considerable line broadening of the 6′-H is consistent with increased dipolar line

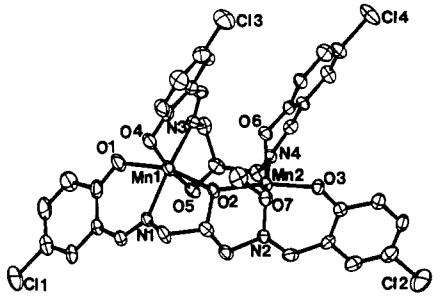

Figure 5. ORTEP diagram of **6** showing the atom-numbering scheme. Important bond lengths and angles are given in ref 14.

broadening due to closer proximity to the Mn center.[11]

One of the interesting features of the dimer spectra is their simplicity. The monomer and dimer spectra contain about the same number of isotropically shifted resonances, yet examination of the structure of the dimer (Figure 5) clearly shows that all four phenolates are chemically and magnetically inequivalent. Therefore, the dimer is dynamic on the NMR time scale. Magnetic equivalence of the phenolates must be achieved by an internal rearrangement of the dimer, since saturation transfer experiments have conclusively demonstrated that the monomer and dimer do not interconvert rapidly on the NMR time scale (vide infra).

No peak is observed that can be assigned to the proton on the 2-C atom of the propane backbone of 2-OH-SALPN in any of the spectra obtained for the dimers. This is likely due to the bonding of the alkoxide to the Mn(III) centers in the dimer and subsequent broadening and/or shifting of the 2-C proton beyond detection limits. These effects are also likely to be involved in rendering the imine C–H and methylene protons unobservable. The imine and methylene protons are two bonds removed from metal-donor atoms in both the monomeric and dimeric complexes, while the 2-C proton is in a similar situation only in the dimers.

The upfield shift of both the 4′- and 5′-H atoms of the phenolate rings is somewhat unexpected. Detailed analysis of the origin of the paramagnetic shifts in analogous high-spin Fe(III) compounds, including complexes of Fe(SALEN)X, have been made.[17-19] The spectra obtained for these materials show an alteration of the sign of the isotropic shift of the phenolate protons. This is consistent with a dominant contact mechanism and spin delocalization in the phenolate π-system. Clearly, different mechanisms are operating in the Mn complexes. Although a detailed analysis of the origins of the observed isotropic shifts in the spectra of the manganese complexes is beyond the scope of the present work, a few general comments are warranted. In general, both dipolar (through space) and contact (through bonds) mechanisms are expected to contribute to the isotropic shifts observed in the NMR spectra of transition-metal ligand protons,[20,21] and neither mechanism can be neglected a priori in the case of d^4 high-spin Mn(III). In the case of Fe(SALEN)X complexes, the dipolar

(17) Pyrz, J. W.; Roe, A. L.; Stern, L. J.; Que, L., Jr. *J. Am. Chem. Soc.* **1985**, *107*, 614.
(18) LaMar, G. N.; Eaton, G. R.; Holm, R. H.; Walker, F. A. *J. Am. Chem. Soc.* **1973**, *95*, 63.
(19) Heistand, R. H., II; Lauffer, R. B.; Fikrig, E.; Que, L., Jr. *J. Am. Chem. Soc.* **1982**, *104*, 2789.
(20) Jesson, J. P. In *NMR of Paramagnetic Molecules*; Lamar, G. N., Horrocks, W. D., Jr., Holm, R. H., Eds.; Academic Press: New York, 1973; p 1.
(21) Bertini, I.; Luchinat, C. *NMR of Paramagnetic Molecules in Biological Systems*; Benjamin/Cummings: Menlo Park, CA, 1986; Chapter 2.
(22) Li, X.; Pecoraro, V. L. *Inorg. Chem.*, in press.
(23) Rotating platinum electrode (RPE) voltammetry samples the properties of the bulk solution since the product of the electrode reaction is continuously swept away. This allows one to establish whether an oxidative or reductive current is passed. In contrast, cyclic voltammetry samples the electroactive species at the electrode surface and does not distinguish a priori whether the original state of the electroactive component was oxidized or reduced. For more details see: Bard, A. J.; Faulkner, L. R. *Electrochemical Methods: Fundamentals and Applications*; Wiley: New York, 1980.

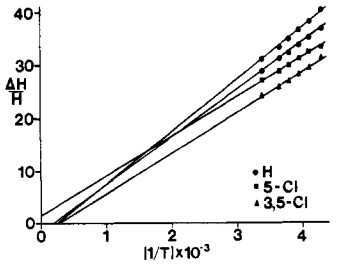

Figure 6. Plot of the paramagnetically shifted resonances of the mononuclear complexes of this study as a function of temperature.

contribution is negligible because of the near-spherical electronic symmetry of the high-spin d^5 ion. Spin density is transferred to the SALEN phenolate ligands via covalent mixing of phenolate and Fe 3d orbitals, as reflected in the energy of the phenolate to Fe(III) charge-transfer transition.[17] This interaction can transfer only down-spin from the ligand to Fe(III), since each metal orbital is singly occupied. The analysis of the Fe(SALEN)X spectrum is straightforward, with the 3′- and 5′-H atoms shifted upfield and the 4′- and 6′-H atoms shifted downfield.[17-19] The delocalization of spin density via the imine onto the phenolate ring leads to an inequivalency between the 4′- and 6′-H atoms, with the 6′-H being shifted only ca. 50–60% the amount of the 4′-H isotropic shift.[18,19]

The situation is more complex for high-spin Mn(III). The proposition that the shifts observed in these complexes are dominated by the contact component is reasonable, given the large distances between the 4′- and 5′-H atoms and the Mn center and the $1/r^3$ distance dependence of the dipolar mechanism.[20,21] This expectation is supported by a lack of significant curvature in the Curie temperature dependence of the spectra over −40 to +23 °C and the near-zero intercepts, which are comparable to those of Fe(SALEN) (±10%, Figure 6).[18,21] Smaller contact shifts, compared to those found for the Fe(III) analogues, are consistent with the reduction of spin density on the metal center and the expected decrease in covalency in the Mn–O,N bonds. However, analysis of the spectra of the Mn(III) complexes in terms of a contact mechanism is complicated by the possibility for transfer of up- or down-spin density from the ligand to Mn(III), by the possible existence of π and σ delocalization mechanisms of similar absolute magnitude for the 3′- and 6′-H atoms, and by the increased importance of delocalization via the imine moiety. Similar types of interaction have been seen for other manganese complexes (in the tripyrazolylhydroborate–manganese dimers,[13] the spectral features could be explained by both delocalization processes depending on the isomer of interest). Delocalization involving transfer of up-spin from the phenolate to Mn(III) would be expected to give rise to alternating shifts that are opposite in sign from those found in the analogous Fe(III) complexes. This does not have a dominant effect since the protons in the 5′-position are still shifted upfield.

The importance of spin delocalization via the imine can be addressed by using complexes that do not contain imines conjugated with the phenolate ring. The spectrum obtained for the manganese(III) complex with ethylenebis((*o*-hydroxyphenyl)-glycine) $[Mn(EHPG)]^-$ contains phenolate resonances that are shifted both upfield and downfield.[22] The monodecarboxylated derivative Mn(EHGS) (EHGS = trianion of *N*-salicylidene-*N*′-((*o*-hydroxyphenyl)carboxymethyl)ethylenediamine) contains one phenolate that is conjugated to an imine and one that is not. In this case, all the resonances from the imino phenolate protons are shited upfield.[22] These data clearly demonstrate that two contact shift pathways are operative, involving spin delocalization via both the imine N-donor and the phenolate O-donor atoms.

Solution Chemistry. The NMR data presented above has been used in conjunction with data from other physical techniques to characterize the solution behavior of a number of manganese complexes of 2-OH-SALPN. These studies reveal a rich solution chemistry that involves conversions between the monomeric cation $Mn(2\text{-OH-SALPN})^+$ and the neutral, alkoxo-bridged dimer

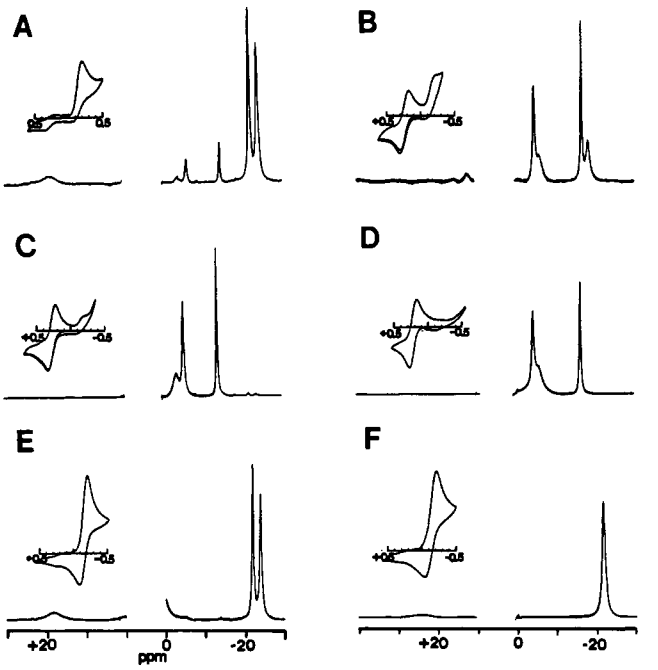

Figure 7. Cyclic voltammograms and paramagnetic NMR spectra for compounds **1**, **2**, and **3**: (A) **1** in methanol; (B) **1** in DMF; (C) **2** in methanol; (D) **2** in DMF; (E) **3** in methanol; (F) **3** in DMF. Conditions of each experiment are given in the text. Deuterated solvents were used for NMR spectra.

Scheme I

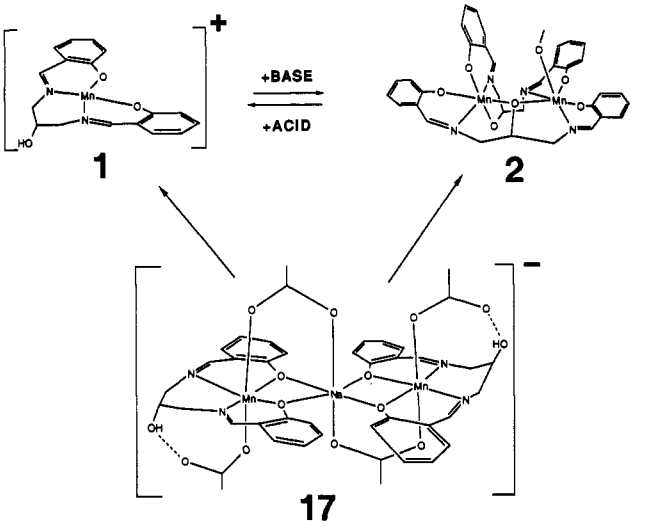

$Mn_2(2\text{-OH-SALPN})_2$ (Scheme I).

The reaction of 2-OH-SALPN with 3 equiv of base and 1 equiv of $Mn(OAc)_3$ produced X-ray-quality crystals of **1**, polymeric $[Mn(2\text{-OH-SALPN})(OAc)]_n$, from DMF. Physicochemical studies of methanol solutions of **1** indicate that it forms the monomeric cationic complex $Mn(2\text{-OH-SALPN})^+$ in this solvent. Methanol solutions of **1** conduct as a 1:1 electrolyte, indicating that the axial acetate ligands are dissociated. The change in the magnetic susceptibility of **1** upon dissolution in methanol is consistent with a weakly antiferromagnetically coupled solid-state material (μ = 4.85 μ_B) forming isolated spin systems in the solution state (μ = 5.01 μ_B). The ^1H NMR spectrum of this compound in methanol reveals the isotropically shifted resonances diagnostic for the presence of the monomeric cation (Figure 2). Peaks due to the presence of a small amount of the dimer are also observed. Cyclic voltammetry of **1** in methanol reveals a Mn(III/II) reduction process at −178 mV. Voltammetry at a rotating platinum electrode confirms this process is a reduction.[23]

The behavior of **1** in DMF is markedly different from that seen in methanol. The reduction seen in methanol is no longer present

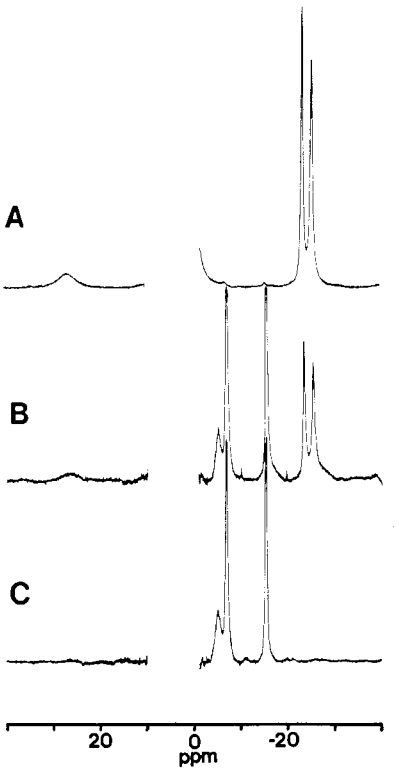

Figure 8. Paramagnetic NMR spectra of (A) compound **3** (B) compound **3** following addition of approximately 0.6 equiv of base, and (C) compound **3** following the addition of 1.0 equiv of base in CD_3OD.

in the cyclic voltammogram of the complex. Instead, a quasireversible oxidation is observed at +230 mV (Figure 7). The nature of this redox process has also been confirmed by using rotating platinum electrode voltammetry. The conductivity of this solution indicates that a nonelectrolyte is present as the major species; therefore, this material is neutral. The solution magnetic susceptibility (μ = 4.63 μ_B) is substantially reduced from the spin-only value (μ = 4.9 μ_B) and from the value obtained from **1** in the solid state (μ = 4.85 μ_B) indicating stronger antiferromagnetic interactions exist between the Mn(III) centers. Examination of the ^{1}H NMR spectrum reveals the resonances characteristic of the alkoxo-bridged dimer Mn_2(2-OH-SALPN)$_2$(DMF) (Figure 7). This DMF solution can be converted to a solution containing the monomeric cation by the addition of methanol (to approximately 30% v/v).

When the five-coordinate complex **3** [Mn(2-OH-SALPN)(NCS)] is dissolved in either methanol or DMF, conductivity measurements show that a 1:1 electrolyte is formed. Both the solid-state and solution-state magnetic susceptibilities (Table II) are consistent with noninteracting high-spin Mn(III) centers. Cyclic voltammetry of **3** in methanol gives the same quasireversible reduction seen for **1** in this solvent (Figure 7). Similarly, the ^{1}H NMR spectrum of **3** contains only the resonances associated with the monomeric cation (Figure 7). Thus, both complexes **1** and **3** form the same monomeric cation in methanol. However, unlike **1**, **3** does not dimerize in DMF, as evidenced by the retention of the physical properties (Tables I–III) and ^{1}H NMR spectrum (Figure 7) diagnostic of the monomer in this solvent. This suggests that a base, the acetate ion, is involved in the deprotonation of the 2-OH group and the formation of the alkoxo-bridged dimer.

That the 2-OH group is irrelevant to the formation of the monomer and essential to the formation of the dimer is confirmed by studies of Mn(III) complexes of the parent ligand, SALPN. The physical properties of **4** ([Mn(SALPN)H_2O]ClO_4) closely resemble those of **3** in all solvents. Complex **4** is known to react aerobically with hydroxide to form a bis(μ-oxo) Mn(IV) dimer.[10] The electronic absorption, IR, electrochemical, and magnetic properties of this dimer are distinct from those of **2**.

The role of acid/base chemistry in the monomer/dimer conversions was explored. When sodium methoxide or tetrabutylammonium hydroxide is added to **3**, the electrochemical and spectroscopic properties of **2** are produced (Figure 8). The conversion is complete upon the addition of 1 equiv of base. Figure 8B illustrates that the features of the NMR spectra originating from the dimer and monomer in mixtures of the two are easily distinguished. The interconversion rate between monomeric and dimeric forms is also slow on the NMR time scale. A saturation transfer experiment involving saturation of resonances associated either with the dimer or with the monomer in a 60:40 mixture of the two failed to show any effect on the corresponding resonances of the species not irradiated. Both cyclic and rotating platinum electrode voltammograms correlate well with the relative integrated intensities of the proton resonances of the two species in mixtures of monomer and dimer. The current observed for the monomeric cation's reduction is twice that observed for the dimer's first oxidation, correlating well with amounts of manganese available for each redox process.

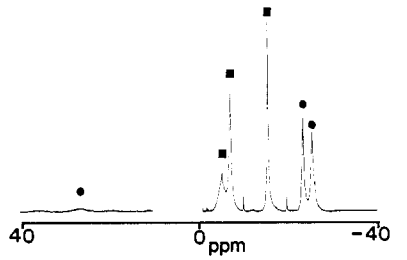

Figure 9. NMR spectrum of **17** in CD_3OD. Peaks marked by ● are from the monomer and peaks marked by ■ are from the dimer.

The dimerization is chemically reversible. Stoichiometric addition of acid returns all of the physical parameters to those of the monomeric cation (Tables I–III). The nature of the acid is of little consequence to either the thermodynamics or kinetics of this process, as aqueous perchloric, aqueous hydrochloric, nonaqueous hydrochloric, and acetic acids all produce the same results. Approximately 1 min is required for the acid dissociation of the dimer.

The ^{1}H NMR studies outlined above have been particularly useful in examining the solution chemistry of the trinuclear cluster **17** ([$NaMn_2$(2-OH-SALPN)$_2$(OAc)$_4$]$^-$) (Scheme I). The solid-state structure of this cluster was described in the previous paper.[14] Examination of the ^{1}H NMR spectrum of the cluster dissolved in CD_3OD reveals that the cluster dissociates and forms both the monomeric cation and the neutral dimer (Figure 9). There is no evidence for bridging acetate ligands, which have methyl proton resonances in the +30 to +50 ppm range in other complexes.[13,24,25] The cyclic voltammogram obtained from a methanol solution of this cluster reveals redox processes that are characteristic of both the monomer and dimer (−145 mV; +230 mV). Therefore, we conclude that the sodium-bridged species is unstable in solution, forming instead the monomeric cation and the dimer **2**. Only the dimer is generated in aprotic solvents such as DMF and methylene chloride.

Electronic absorption spectroscopic parameters for the isolated complexes in this study are reported in Table IV. Each compound displays an intense ligand-to-metal charge-transfer transition (LMCT) in the 360–400-nm region (ϵ = 6000–20 000 M^{-1} cm^{-1}) that may be assigned[26] to the phenolate to Mn(III) LMCT. No other chromophore present is expected to give rise to intense transitions in the visible region. A small shoulder may be observed in the electronic absorption spectra of some of the Mn complexes at ca. 550 nm (ϵ = 300 M^{-1} cm^{-1}), which most likely arises from a d–d transition. The dimerization process can also be followed spectroscopically and confirms the stoichiometry of the acid/base reactions. The characteristic green color of the monomer converts to a golden brown with a concomitant increase in intensity upon

(24) Li, X.; Kessissoglou, D. P.; Bender, C. A.; Bonadies, J. A.; Maroney, M.; Pecoraro, V. L. Manuscript in preparation.
(25) Kessissoglou, D. P.; Lah, M. S.; Kirk, M. L.; Bender, C. A.; Pecoraro, V. L. *J. Chem. Soc., Chem. Commun.* **1989**, 84.
(26) Patch, M. G.; Carrano, C. J. *Inorg. Chim. Acta* **1981**, *56*, L71.

formation of the dimer. The visible absorption change associated with the dimerization process for the unsubstituted complexes is a shift in the maximum absorbance from 383 to 375 nm (in MeOH), with an isosbestic point at 399 nm.

Redox Chemistry of Mn_2(2-OH-SALPN)$_2$(solvent). The redox chemistry of the dimer **2** was explored further in acetonitrile, a solvent that allows more positive potentials to be employed than are accessible in methanol. In acetonitrile, anodic waves are observed at +280, +1200, and +1600 mV. The broad, irreversible oxidation wave observed at ca. +1200 mV is assigned to a ligand-centered oxidation based on studies of the free ligand, which undergoes oxidation at +1100 mV. The oxidation at +1600 mV is also irreversible and is likely a second metal-base oxidation (vide infra). Full quantitation of this wave was not possible, as the preceding ligand oxidation quickly passivates the electrode surface.

The quasireversible oxidation process at +280 mV (+314 mV in MeOH) was examined in more detail. Electrolysis at +400 mV in acetonitrile required one electron per dimer, corresponding to the formal oxidation of one Mn(III) to Mn(IV). A cyclic voltammogram of this solution was identical with one obtained prior to the electrolysis, with the exception that reductive current, rather than oxidative current, was passed on the wave centered at +240 mV. This indicates that the oxidized product is stable over the course of the electrolysis. Indeed, the entire process may be reversed by passing the same amount of current at 0 mV, regenerating the original cyclic voltammetric behavior.

NMR and cyclic voltammetry reveal that the oxidized product has a range of stabilities depending upon the solvent. When the oxidation is performed in methanol, loss of the quasireversible redox couple occurs in a few hours. In DMF, the couple persists for several days, while in acetonitrile it is unchanged after 8 days. The structure, physical properties, and reactivity of these oxidized species are currently being investigated.

The structure and electrochemical properties of the mononuclear Mn(IV) complex Mn(SALADHP)$_2$ have been reported previously[27] [SALADHP = dianion of 2-methyl-2-(salicylideneamino)-1,3-dihydroxypropane]. This Mn(IV) ion is six-coordinate with a coordination sphere that is almost identical with that of Mn1 in Figure 5 with the following two exceptions. First, both of the alkoxide donor oxygens in the mononuclear case have distances of 1.87 Å, while Mn1–O2 is very long (2.317 Å) due to a Jahn–Teller distortion. Second, and more important, O2 is a bridge between Mn1 and Mn2 in the dimer. The shift in oxidation potential between Mn(SALADHP)$_2$ and Mn1 of the dimer is dramatic. A reductive wave at −460 mV is observed for the monomer, while an oxidative wave at +230 mV occurs for Mn1. Thus, the strong Mn2–O2 bond (1.90 Å) destabilizes the Mn(IV) oxidation state by nearly 700 mV.

The Mn2 coordination sphere in the dimer is similar to the environment of the Mn(III) ions in [Mn(DALAP)DMF]$_2$ [DALAP = 2,6-bis(((2-hydroxyphenyl)imino)methyl)-4-methylphenol].[28] The primary differences are that DMF replaces methanol, the Mn–Mn separation is 6.8 Å (rather than 3.8 Å as in **6**), and the alkoxide is replaced by a phenolate, which does not form a bridge between the two Mn(III) ions in [Mn(DALAP)DMF]$_2$. An oxidation of the DALAP dimer occurs at +1700 mV in DMF. By analogy, we assign the wave at +1600 mV in the cyclic voltammogram of **3** to oxidation of Mn2.

Summary

The coordination chemistry described in this account clarifies the seemingly disparate behavior reported for manganese complexes of SALPN and 2-OH-SALPN. While both ligands form monomeric Mn(III) species in solution, bound in the classic tetradentate bis(imino phenolate) geometry, the chemistry in basic media is very different. The [Mn^{IV}(SALPN)(μ-O)]$_2$ dimer forms quantitatively in basic solution. Addition of acid yields the original [Mn^{III}(SALPN)]$^+$ and hydrogen peroxide.[10] In contrast, the participation of the 2-OH moiety of (2-OH-SALPN) leads to the isolation of the alkoxy-bridged Mn(III) dimer [Mn^{III}_2(2-OH-SALPN)$_2$(solvent)]·solvent. When acid is added to a solution of this material, clean conversion to the monomeric cation, without the formation of hydrogen peroxide, is accomplished.

The NMR spectra of [$NaMn_2$(2-OH-SALPN)$_2$(OAc)$_4$]$^-$ demonstrate the power of NMR spectroscopy in establishing the speciation of loosely associated manganese clusters. This cluster is unstable in methanol and DMF, preferentially forming monomer and dimer. In contrast, we report in a separate contribution the ^{1}H NMR spectra of mixed-valence trinuclear manganese clusters[24] and demonstrate that these materials retain their integrity in chloroform and DMF, while they dissociate in methanol. Thus, the judicious application of NMR spectroscopy can establish the solution conditions where a manganese cluster of interest can be examined intact.

Finally, we can relate these complexes to the OEC. In addition to manganese, calcium is an essential metal for water oxidation in the photosynthetic reaction center.[29] Recently, it has been proposed that calcium may be involved in a structural role that stabilizes a manganese cluster.[25,30] This interaction could occur via direct bridging ligands as is observed in the X-ray structure of Mn–Ca concanavalin A.[31] In addition to a structural role, calcium might also function to fine tune the redox potential of a manganese cluster. The comparison of the redox potentials between [Mn^{III}_2(2-OH-SALPN)$_2$(CH_3OH)]·CH_3OH and Mn^{IV}(SALADHP)$_2$ illustrates how the use of one alkoxide oxygen as a bridge between two metals can destabilize the Mn(IV) oxidation level by 700 mV. Although it would be more difficult to generate an oxidized cluster, once formed, it would be a much more highly oxidizing center. The initial oxidation could easily be accomplished by the strong oxidant Y_z^+, which is available in the reaction center. The incorporation of a divalent metal into this site would be expected to cause a less dramatic, yet still significant, shift in the potential. A Ca(II) ion is preferential to Mn(II) in this capacity since calcium is redox inert. Thus, a biological Mn^{IV}–O–Mn^{II} site might conproportionate to Mn^{III}–O–Mn^{III} rather than achieve the more highly oxidizing center based on an Mn^{IV}–O–Ca^{II} cluster. Studies to evaluate this hypothesis are under way.

Acknowledgment. We wish to acknowledge the National Institutes of Health for support of this research through Grants GM39406 to V.L.P. and GM38829 to M.J.M. Support for a postdoctoral research fellowship from the Program for Protein Structure and Design to J.A.B. is gratefully acknowledged. We wish to thank Steven Brocchini and Frank Parker for their technical assistance in collecting NMR spectra.

Registry No. **1**, 39708-64-0; **2**, 120204-54-8; **3**, 120204-38-8; **4**, 86773-55-9; **5**, 120204-35-5; **6**, 120204-52-6; **7**, 120204-36-6; **8**, 120204-53-7; **9**, 120204-37-7; **10**, 120204-51-5; **11**, 120204-39-9; **12**, 120229-17-6; **13**, 120204-42-4; **14**, 120229-16-5; **15**, 120204-40-2; **16**, 120229-15-4; **17**, 120204-41-3; Mn_2[2-OH(4-OMe-SAL)PN]$_2$·DMF, 120204-50-4; Mn_2[2-OH(5-OMe-SAL)PN]$_2$·DMF, 120204-49-1; Mn_2[2-OH(6-OMe-SAL)PN]$_2$·DMF, 120204-48-0; Mn_2(2-OH-SALPN)$_2$·DMF, 120204-47-9; Mn_2[2-OH(5-Cl-SAL)PN]$_2$·DMF, 120204-46-8; Mn_2[2-OH(3,5-Cl_2-SAL)PN]$_2$·DMF, 120204-45-7; Mn_2[2-OH(5-Br-SAL)PN]$_2$·DMF, 120204-44-6; Mn_2(2-OH-SALPN)$_2$·MeCN, 120204-56-0; Mn_2[2-OH(5-Cl-SAL)PN]$_2$·MeCN, 120204-55-9; Mn_2[2-OH(5-Br-SAL)PN]$_2$·MeCN, 120204-57-1; Mn(SALEN)$^+$, 47111-14-8; Mn(2-OH-SALPN)$^+$, 120204-43-5.

Supplementary Material Available: Electrochemical properties (Table SIII) and UV–visible spectroscopic properties (Table SIV) for all of the complexes of this study (4 pages). Ordering information is given on any current masthead page.

(27) Kessissoglou, D. P.; Li, X.; Butler, W. M.; Pecoraro, V. L. *Inorg. Chem.* **1987**, *26*, 2487.
(28) Pecoraro, V. L.; Li, X.; Baker, M. J.; Butler, W. M.; Bonadies, J. A. *Recl. Trav. Chim. Pays-Bas* **1987**, *106*, 221.
(29) Carumarata, K.; Chenaie, G. M. *Plant Physiol.* **1987**, *84*, 587.
(30) Ghanotakis, D. F.; Topper, J. N.; Babcock, G. T.; Yocum, C. F. *FEBS Lett.* **1984**, *170*, 169.
(31) Hardman, K. D.; Ainsworth, C. F. *Biochemistry* **1972**, *11*, 4910.